
DATA-JUICER SANDBOX: A COMPREHENSIVE SUITE FOR MULTIMODAL DATA-MODEL CO-DEVELOPMENT

Daoyuan Chen*, Haibin Wang*, Yilun Huang*, Ce Ge, Yaliang Li[†], Bolin Ding, Jingren Zhou
Alibaba Group

{daoyuanchen.cdy, binke.whb, lielin.hyl, gece.gc}@alibaba-inc.com
{yaliang.li, bolin.ding, jingren.zhou}@alibaba-inc.com

ABSTRACT

The emergence of large-scale multi-modal generative models has drastically advanced artificial intelligence, introducing unprecedented levels of performance and functionality. However, optimizing these models remains challenging due to historically isolated paths of model-centric and data-centric developments, leading to suboptimal outcomes and inefficient resource utilization. In response, we present a novel sandbox suite tailored for integrated data-model co-development. This sandbox provides a comprehensive experimental platform, enabling rapid iteration and insight-driven refinement of both data and models. Our proposed “Probe-Analyze-Refine” workflow, validated through applications on state-of-the-art LLaVA-like and DiT-based models, yields significant performance boosts, such as topping the VBench leaderboard. We also uncover fruitful insights gleaned from exhaustive benchmarks, shedding light on the critical interplay between data quality, diversity, and model behavior. With the hope of fostering deeper understanding and future progress in multi-modal data and generative modeling, our codes, datasets, and models are maintained and accessible at <https://github.com/modelscope/data-juicer/blob/main/docs/Sandbox.md>.

1 INTRODUCTION

The advent of multi-modal generative models has revolutionized artificial intelligence, pushing the boundaries of functionality and creativity across various domains (OpenAI, 2024a;b; Wang et al., 2024). Recognizing the pivotal role of training data in shaping model performance, there are fast-growing efforts to curate datasets of larger scales and higher quality (Jakubik et al., 2024).

However, the development trajectories of these models and datasets have historically diverged, guided more by intuition than by systematic co-development methodologies. Recent advances in enhancing multi-modal generative models tend to be either model-centric or data-centric, rarely bridging the two aspects cohesively. For example, model-centric methods focus on algorithmic enhancements and architectural innovations under fixed data priors, while data-centric strategies usually concentrate on processing and cleaning datasets independently of specific model training contexts (Qin et al., 2024). Both approaches usually suffer from a lack of systematic guidance and cooperative synergy, relying heavily on heuristic exploration and single-perspective expertise. This fragmented landscape presents a significant barrier to achieving optimal model performance, as the interplay between data characteristics and model capabilities remains largely underexploited.

Moreover, the practical implementation of multi-modal generative models is further complicated by infrastructure constraints, escalating computational costs, and the accelerating pace of development cycles (Xu et al., 2024b). In the age of large-scale models with rapidly growing model parameters and dataset sizes, the processes of data processing and model training become increasingly resource-intensive, demanding substantial time and computations. Due to the absence of cost-effective platforms that simplify and speed up data-model co-development, researchers and developers often face the dilemma of prioritizing result-driven development at the expense of thorough, insight-led

*These authors contributed equally to this work.

[†]Corresponding author.

exploration. This deficiency hinders the iterative refinement for both domains, leading to sub-optimal outcomes as improvements in one domain are hard to inform, apply and enhance each other directly.

To fill this gap, we introduce the Data-Juicer Sandbox, a comprehensive suite for facilitating the co-development of multi-modal data and generative models. Building upon an open-source data processing system tailored for multi-modal generative models, Data-Juicer (Chen et al., 2024a), our sandbox suite further integrates a wealth of off-the-shelf components optimized for usability and compatibility with existing model-centric infrastructures. Collectively, it offers flexibly customizable orchestration from different levels including end-to-end workflows, specific development behaviors, and underlying data-model development capabilities. Within the sandbox laboratory, users are empowered to rapidly explore different data pipelines and model configurations on cost-controlled datasets and models. This accelerates the discovery of insightful patterns and informed decision-making, ultimately paving the way for scalable, resource-efficient data-model development.

To exemplify the efficacy of our sandbox, we propose a “Probe-Analyze-Refine” workflow, meticulously crafted to explore the synergies between data processing operators, target model metrics, and the scalability of these enhancements. We apply this workflow to two cutting-edge models: Mini-Gemini (Li et al., 2023), an LLaVA-inspired model for image-to-text generation, and EasyAnimate (Xu et al., 2024a), a Diffusion Transformer based model for text-to-video generation. Thanks to the sandbox’s capabilities, we attain significant advancements in data quality and model performance, such as achieving top spot on the VBench (Huang et al., 2024) leaderboard, outperforming strong competitors such as VideoCrafter (Chen et al., 2024b) and AnimateDiff (Guo et al., 2024). These achievements are underpinned by a series of insights linking 31 data processing operators and 35 model metrics, including analysis of the fine-grained impact of data processing for model training, the delicate balance between data diversity and model performance, and the strategic optimization of data scaling for enhanced model-data co-development.

Our contributions can be summarized as follows:

- **Innovative Sandbox Suite:** To the best of our knowledge, this is the first open-source sandbox suite tailored for co-development between multi-modal data and generative models, rendering experimental exploration in this field more insightful, systematic, convenient and reusable.
- **Effect-Proven Workflow:** We present a new progressive workflow for data-model co-development and substantiate its impact through extensive empirical evidence such as achieving new top-tier performance in image understanding and video generation tasks.
- **Practical Guidance:** We conduct extensive experiments on benchmarking the effects of dozens of data processing operators and model metrics, providing fruitful and valuable insights toward further advancements in multi-modal generative models.

2 RELATED WORKS

Model-Centric Progress in Multimodal Generative Models. Multimodal generative models have captivated researchers with their formidable capabilities (OpenAI, 2024a;b), leading to a surge in model-centric development efforts. These focuses mainly lie in refining training algorithms (Caffagni et al., 2024; Li et al., 2024; Zhang et al., 2024), advancing model architectures and components (He et al., 2024a; Yin et al., 2024; Jiao et al., 2024), and harnessing the models’ generative potential for various applications (Wang et al., 2024; Liu et al., 2024a; Zhou et al., 2024). There is a growing consensus that transformer-based scaling is predominant (Xu et al., 2023). However, the high computational requirements imposed by scaling laws (Xu et al., 2024b) and the optimization challenges inherent to generative models (Manduchi et al., 2024) often confine insights to specific datasets or vague data characteristics. This situation leaves a significant gap in comprehending the extent to which models’ performance and behavior hinge upon implicit assumptions and inductive biases embedded within the underlying data distributions.

Trends in Data-Centric Development for Multimodal Generative Models. An emerging trend shifts the focal point from models to data (Jakubik et al., 2024; Bai et al., 2024), underscored by the notion that large models function akin to data compressors (Delétang et al., 2024). Echoing the principle of “garbage in, garbage out”, meticulous data processing is recognized as pivotal. Efforts now isolate data manipulation as a primary experimental variable in multimodal generative modeling

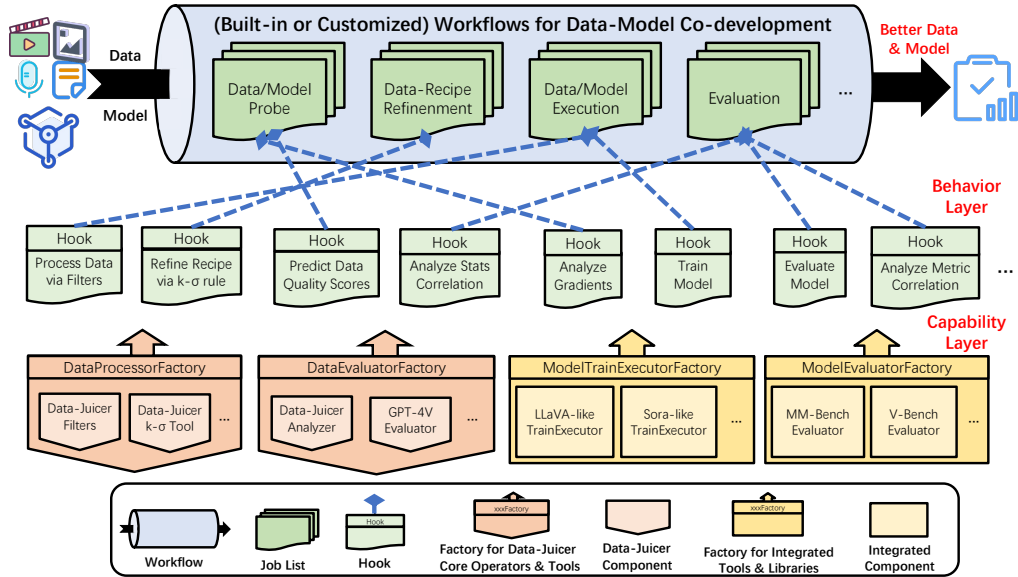


Figure 1: Overview of the Data-Juicer Sandbox Laboratory. Here, *Probe Jobs* conduct preliminary analyzes on both data and models. Based on the insights gleaned from probe results, *Refine-Recipe Jobs* optimize data processing recipes and *Execution Jobs* subsequently undertake the core tasks of data processing, model training, and inference. Lastly, *Evaluation Jobs* serve to critically appraise the resultant data quality and model effectiveness. These four stages proceed in a methodical sequence, with each step offering versatile customization through configuration options at diverse granularity across the data-model co-development lifecycle: end-to-end workflows, generic behaviors, and foundational capabilities.

(He et al., 2024b). Nonetheless, multimodal data processing involves highly heterogeneous processing workflows, vast quantities, diverse types, and the high cost of training downstream models. This complexity results in predominantly heuristic approaches, such as data filtering and synthesis guided by human intuition (Long et al., 2024). There remains a huge exploration space for more systematic data development methodologies and their harmonious integration with model development.

Open-Source Infrastructure for Multimodal Generative Model Development. The ecosystem has flourished with robust infrastructure for multimodal model development, including frameworks for training and evaluation like Transformers (Wolf et al., 2020), Diffusers (von Platen et al., 2022), NeMo (Harper et al.), MMagic (MMagic Contributors, 2023), ESPNNet (Peng et al., 2023), MMBench (Liu et al., 2024b) and *etc.* Regarding multimodal data infrastructure, contributions are mainly in the form of datasets and dataset-specific preprocessing scripts, such as DatasetsHub from HuggingFace (Lhoest et al., 2021). The practical wisdom and foundational capabilities in data processing often remain unstandardized and underleveraged. Existing data processing frameworks, mainly tailored for single-modal data (Computer, 2023; Bradski, 2000; Hwang et al., 2023), highlight the nascent stage of systematic multimodal data development platforms (Chen et al., 2024a; Du et al., 2023). Recognizing the reciprocal relationship where large, high-quality datasets facilitate superior models, which in turn can aid in generating more refined datasets, our work introduces a dedicated intermediary layer. By seamlessly integrating state-of-the-art model-centric multimodal infrastructure with the Data-Juicer system, we enable streamlined, insight-driven co-development between models and data.

3 THE PROPOSED DATA-JUICER SANDBOX LABORATORY

3.1 MOTIVATION AND DESIGN

Why do we need data-model co-development? In the era of large models, the development of both data and models necessitates a collaborative approach involving numerous algorithm researchers

and system engineers. Training data for large models is often highly heterogeneous in terms of quality, context, type, and timeliness. The processing and mixing (Ge et al., 2024) of these datasets, known as data recipes, are complex and varied. The scale of data amplifies the stakes for refinement attempts on both data and models, imposing substantial computational and time burdens. Traditional data-centric or model-centric strategies fall short by optimizing in isolation, leading to *diminished overall efficiency and resource misallocation*. When either component requires adjustment, the dual optimization challenge inflates costs, as one part may have already reached near-optimal status.

Why do we need a sandbox laboratory? Given the high cost associated with iterative development, existing methods often resort to heuristic approaches for improving data or models. For example, scaling up “cleaned” datasets can be problematic because determining what constitutes a “clean” dataset and measuring its quality qualitatively remains a challenge. Furthermore, the impact of iterations on data and models is difficult to attribute due to numerous influencing factors and the considerable engineering effort required. Therefore, more insightful solutions are needed for data-model co-development.

A unified sandbox environment offers controlled experimentation with low overhead, high transferability, and guided optimization. It permits users to swiftly iterate and optimize data recipes using cost-controlled datasets and models, with insights readily scalable to full-scale production environments, thus addressing larger computational demands of data processing and model training.

The three-layer orchestration of Data-Juicer sandbox. To accommodate the multifaceted workflows intrinsic to data-model co-development, we design a versatile, user-friendly sandbox laboratory, as depicted in Figure 1. The laboratory incorporates a spectrum of components for activities such as data analysis, filtering, recipe optimization, model training, inference, and evaluation, all orchestratable via configuration files. The architecture is stratified into three tiers: bespoke end-to-end **workflows**, generic development **behaviors**, and foundational data-model development **capabilities**:

- The top tier delineates co-development workflows executed sequentially across four phases: probing data/models, refining data recipes, executing data/model operations, and evaluation. The sequence of tasks within each phase is adjustable through an input configuration file, permitting users to leverage pre-established and effect-proven workflows or customize their own with ease.
- Moreover, users can flexibly introduce or innovate components at the capabilities level (such as novel models, metrics, or data processing algorithms) and behavior hooks (like multidimensional data quality assessments and adaptive adjustments based on multiple probe outcomes) interchangeably.

This design allows for streamlined configuration and reuse of established infrastructure. Importantly, it expedites the prototyping of data and model development solutions, integrating actionable and quantifiable capabilities for swift feedback derivation and informed decision-making. Detailed explorations of the lower tiers are provided in Section 3.2, while Section 3.3 showcases the sandbox’s utility in establishing a probe-refine-scaling workflow for data-model co-development.

3.2 FLEXIBLE CAPABILITY FACTORY AND BEHAVIOR HOOKS

Components for Advanced Data Processing. Within the sandbox, we design numerous factory classes and behavior hooks for data processing and evaluation, simplifying and unifying the interfaces provided by the open-source Data-Juicer system (?). Users gain great flexibility to leverage over 100 feature-rich operators and dedicated tools for efficient data analysis, processing (including filtering, modifying, generating, *etc.*), and evaluation:

- From an actionable perspective, key components include *DataProcessors* and *DataRecipeRefiners*. *DataProcessors* invoke off-the-shelf data processing operators from Data-Juicer, such as *Filters* and *Mappers*, enabling accelerated and scalable data processing through system optimization and parallel support. *DataRecipeRefiners* offer tools to refine recipe configurations, such as adjusting filtering thresholds based on k-sigma principle or percentile distribution to differentiate data subsets.
- From a measurable perspective, *DataAnalyzers* and *DataEvaluators* are provided. *DataAnalyzers* encapsulate various data analysis tools from Data-Juicer, performing efficient computations of target metrics like text perplexity or video aesthetic value, and providing common statistical values

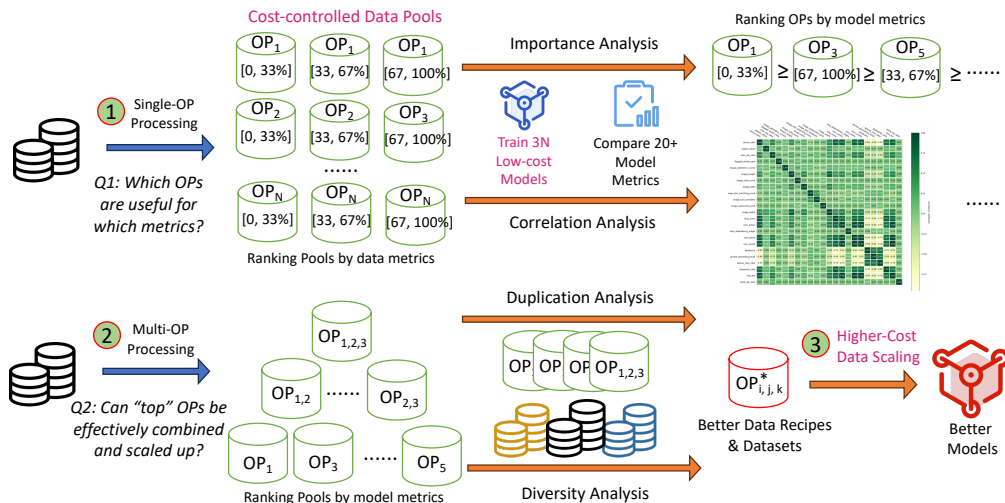


Figure 2: A probe-analyze-refine workflow within the sandbox for systematic data-model co-development. (1) The process begins with cost-effective, contrastive explorations on small data pools to identify the most effective data processing operators (OPs). (2) These OPs are then combined and scaled within data recipes through hierarchical data pyramids to assess their cumulative impact on model performance. (3) Lastly, data utilization is optimized via duplication and diversity analysis, guiding the final formulation of refined data recipes and datasets for enhanced large-scale training. This structured workflow enables informed decision-making and efficient optimization for developing superior models.

(mean, variance, percentile thresholds). DataEvaluators include tools for evaluating data quality, such as GPT quality classifier.

Components for Streamlined Model Advancement. Similarly, model development components integrate state-of-the-art open-source tools and libraries, streamlining interfaces and enhancing usability for rapid and user-friendly development experiences. Actionable components encompass training functionalities, such as Mini-Gemini (Li et al., 2023) for image-to-text, EasyAnimate (Xu et al., 2024a) for text-to-video, and ModelScope¹ for general generative models. Measurable components offer evaluation interfaces like FVD (Unterthiner et al., 2019), VBench (Huang et al., 2024) for synthesized video assessment, GPT-4 (OpenAI, 2023) for generated text scoring and ranking, and TextVQA (Singh et al., 2019), MMBench (Liu et al., 2023), and MME (Fu et al., 2023) for image-to-text synthesis evaluation.

Model integration is facilitated through the use of subprocesses to call bash scripts of integrated libraries, with code and parameter adjustments ensuring a cost-controlled environment where, for example, a single GPU card can complete a training session within one day, providing rapid feedback.

3.3 A PROBE-ANALYZE-REFINE WORKFLOW FOR DATA-MODEL CO-DEVELOPMENT

To demonstrate the usage of the sandbox laboratory, here we elucidate a built-in systematic workflow. As illustrated in Figure 2, we commence with a series of cost-effective contrastive explorations aimed at addressing several key questions, before judiciously applying them to enhance large-scale data-model co-development:

1. Initially, we seek to ascertain *which data processing operators (OPs) contribute most effectively to enhancing specific target model metrics?* This involves creating equal-size data pools, each processed uniquely by a singular OP and subsequently ranked by data metrics. Models are trained on these data pools, enabling us to perform an in-depth analysis of OP effectiveness and its correlation with model performance across various quantitative and qualitative indicators.

¹<https://github.com/modelscope/modelscope>

2. Guided by insights derived from the most impactful OPs that ranked highest by model metrics, we proceed to study *whether these OPs can be effectively combined into data recipes and scaled up*. To facilitate this exploration, we establish a hierarchical data pyramid, wherein data pools are categorized across different tiers based on their ranked model metric scores. This stratification also elucidates the viability of OP combinations when scaled with increased data volumes.
3. Finally, we delve into optimizing data utilization through a dual analysis focusing on *duplication* and *diversity*. We will assess whether the training process would benefit more from the repeated use of high-quality data pools or from the inclusion of lower-quality data to expand the overall data pool. Through a systematic examination of cost-controlled experiments, we can formulate optimized data recipes and datasets, which are then leveraged in more resource-intensive training sessions to cultivate models with superior performance.

3.3.1 SINGLE-OPERATOR DATA POOLS

Data-Juicer provides a rich assortment of OPs tailored for multimodal data encompassing text, images, videos, and audio. Given the variability in data sources, models, and downstream tasks, it is imperative to initially ascertain the impact of each OP to guide the optimization of data-model co-development effectively.

To this end, starting with an initial dataset \mathcal{D} , we define a single-operator data pool \mathcal{P}_i as the dataset processed exclusively by the i -th OP (\mathcal{OP}_i) available in Data-Juicer as follows:

$$\mathcal{P}_i = \mathcal{DJ}[\mathcal{OP}_i(\rho_i)](\mathcal{D}), \quad (1)$$

where \mathcal{DJ} denotes the data-processing function implemented by Data-Juicer, and ρ_i is the hyper-parameters governing the operation of \mathcal{OP}_i . The OPs of Data-Juicer can compute specific statistics for every data pools, and apply threshold criteria to selectively filter or modify the data based on these statistics. Within this workflow, the initial dataset \mathcal{D} into three equal-sized segments for filter OPs: $\mathcal{P}_{\text{high}}$, $\mathcal{P}_{\text{middle}}$ and \mathcal{P}_{low} , representing data with high, moderate, and low statistical measures, respectively. A randomly sampled $\mathcal{P}_{\text{random}}$ serves as a control group. This stratification fosters discriminative insights across varying degrees of data processing intensity.

Subsequently, models are trained independently on each data pool, undergoing comprehensive evaluation across multiple performance metrics. Throughout the training, we uphold consistent hyper-parameters and ensure $\mathcal{P}_{\text{random}}$ is of substantial size to yield a reliable and robust average performance across all downstream tasks. This setup enables the identification of best-performing OPs that universally excel or excel under specific evaluation criteria.

Importantly, we adhere to a cost-conscious design, implementing strategies to curtail expenses, such as downsizing the data pools, limiting training iterations, or adopting efficiency-enhancing techniques like LoRA (Hu et al., 2021). It enables the entire experimental pipeline to conclude at an affordable level. Specifically, all of our experiments can be completed within a single day utilizing a single A100 GPU, remaining both feasible and scalable for broader adoption in data-model co-development endeavors.

3.3.2 MULTI-OPERATORS DATA POOLS

Having explored the individual impact of each OP, our next step logically progresses to understanding the dynamics when multiple OPs are sequentially applied as in a data “recipe”. Our aim is to discern whether these OPs complement or counteract each other’s effects. To achieve this, we extend the data pool construction methodology from previous individual OP scenarios to a sequence of OPs:

$$\begin{aligned} \mathcal{P} &= \mathcal{DJ}[\mathcal{OP}_1(\rho_1), \mathcal{OP}_2(\rho_2), \dots, \mathcal{OP}_i(\rho_i)](\mathcal{D}) \\ &= \mathcal{DJ}[\mathcal{OP}_1(\rho_1)](\mathcal{D}) \cap \mathcal{DJ}[\mathcal{OP}_2(\rho_2)](\mathcal{D}) \cap \dots \cap \mathcal{DJ}[\mathcal{OP}_i(\rho_i)](\mathcal{D}). \end{aligned} \quad (2)$$

The number of possible multi-OP data pools grows exponentially with the addition of each new OP, necessitating a strategic selection of combinations to explore. Drawing on insights from single-OP experiments, we propose a pragmatic strategy: combining “Top” OPs, those with progressively diminishing impacts on model performance, while incrementally increasing the number of combinatorics.

Furthermore, we integrate the analysis of inter-OP relationships into our recipe formulation. Our workflow accommodates two approaches:

- The first method entails computing the Pearson correlation coefficients between the statistics generated by these OPs. Using a hierarchical clustering algorithm, we group the OPs into k clusters. From each cluster, we select the OP with the strongest performance to form potential combinations.
- Alternatively, leveraging the outcomes of single-OP tests, we calculate the Pearson correlation coefficients for each dimension within the evaluation metrics. Hierarchical clustering is again utilized to categorize the metrics into k classes. The top-performing OP from each class is chosen to create the combinations. This approach allows us to investigate whether these combinations result in concurrent improvements or mutual inhibition across the evaluative metrics.

In alignment with our methodology for single-OP data pools, we consistently train and evaluate models for each selected multi-OP data pool, while ensuring the process remains cost-effective.

3.3.3 PYRAMID-SHAPED DATA POOLS

Incorporating a greater number of OPs in a recipe may lead to enhanced data quality; however, as per Equ. (2), the resultant data pool volume decreases exponentially with each additional OP. This phenomenon prompts a critical investigation: should we prioritize reusing high-quality data or incorporate lower-quality yet more abundant data to escalate training dataset sizes?

To encapsulate this inherent trade-off between data scale and quality, we devise a hierarchical pyramid architecture for data pools. Given k “top” OPs, we can create $2^k - 1$ combinations of these OPs, as depicted in the left-bottom area in Figure 2. For example, the combination of 3 OPs, $\mathcal{OP}_{1,2,3}$, resides at the highest level of the hierarchy but results in the smallest data pool after Data-Juicer data processing. The combinations of 2 operators, such as $\mathcal{OP}_{1,2}$, are placed at a lower level, and the resulting data pool encompasses that of $\mathcal{OP}_{1,2,3}$ is several times larger in volume. Leveraging findings from Section 3.3.2, we can pinpoint the optimal OP combinations within this pyramid structure. Progressing downward through the pyramid, data pools exhibit a descending average OP ranking (potentially indicative of reduced data quality) alongside an increase in volume.

To reconcile the desire for larger datasets without compromising quality, we devise two experimental strategies built upon this data pyramid: (1) iterative model training with data repetition from the top-layer (highest-quality) data pools, and (2) non-repetitive training incorporating progressively lower-quality, larger-volume data pools from the lower-layer pools. Specifically, we extract a predetermined quantity of data from the top-layer pool for iterative training with variable repetition rates. In parallel, as a baseline, we assemble a non-repeating dataset by consolidating pools from the upper to lower pyramid levels to match the size of the iterated dataset.

These comparative studies enable us to qualitatively assess the efficacy of data reuse versus the inclusion of suboptimal data within a fixed dataset size. Notably, all data pools are uniformly sampled from the original dataset \mathcal{D} , ensuring that the relative proportions of pyramid data pools remain consistent as \mathcal{D} expands. Thus, insights garnered from these experiments can be extrapolated to larger-scale data contexts, informing efficient scaling of data-model co-development practices.

4 PRACTICAL APPLICATIONS

In this section, we illustrate the application of the Data-Juicer sandbox in two distinct scenarios, demonstrating its versatility and effectiveness in enhancing multimodal data-model co-development. These examples instantiate the behavior hooks and capability classes detailed in Section 3.2, following the workflow outlined in Section 3.3. Subsequently, Section 5 delves into the primary findings and insights derived from these two practical scenarios.

4.1 IMAGE-TO-TEXT GENERATION

Our first task focuses on foundational image understanding ability, by experimenting on Mini-Gemini (MGM-2B), a state-of-the-art (SOTA) 2 billion parameter multimodal LLM (Li et al., 2023). The training protocol for MGM-2B involves two stages: pretraining and fine-tuning. Our experimental focus lies in the pretraining phase, which seeks to harmonize visual and textual representations. We utilize the original pretraining dataset, consisting of approximately 1,226k instances, as our original dataset \mathcal{D} . The single-OP and multi-OP data pools are capped at a maximum of 200k

instances, ensuring consistency in training samples. The fine-tuning dataset is sampled to match the down-sampling rate used during pretraining, resulting in a 240k instance subset.

After the two-stage training, model evaluation is conducted on established benchmarks such as TextVQA (Singh et al., 2019), MMBench (Liu et al., 2023), and MME (Fu et al., 2023). Our experimentation encompasses 22 text-image relevant OPs from Data-Juicer, split evenly between text-only and image-related multimodal OPs. For multi-OP data pools, we identify the top-3 performing OPs for all possible combinations. Additionally, we analyze the correlations among the 23 data statistics produced by 22 OPs capable of generating instance-level stats. Employing a hierarchical clustering algorithm, these OPs are grouped into three clusters based on correlation coefficients, with the highest-performing OP from each cluster selected for combination testing.

From these experiments, we identify the optimal OP combination, noting that due to filtering, the final instance count reduces to approximately 159k. These data are then repeated in increments from double up to eightfold, mirroring the size of the original pretraining set. Concurrently, we adopt the methodology from Section 3.3.3 for comparative experiments. The outcomes yield lots of profound insights into image-to-text model training, data processing, and iteration strategies from a data-model co-development perspective.

4.2 TEXT-TO-VIDEO GENERATION

For the second task, text-to-video generation, we adopt the advanced DiT-based EasyAnimate (Xu et al., 2024a) model, which integrates diverse datasets totaling 1,217k instances from InternVid (Wang et al., 2023b) (606k), Panda-70M (Chen et al., 2024c) (605k), and MSR-VTT (Xu et al., 2016) (6k). Baseline experiments are executed on a subset of 40k instances, employing LoRA (Hu et al., 2021) for efficiency. Model outputs are assessed using VBench (Huang et al., 2024) across 16 metrics on video quality and video-text matchness.

Our investigation covered 21 OPs, including 13 text-only OPs and 10 video-related multimodal OPs. Analogous to the image-to-text generation, we conduct single-OP and multi-OP combination experiments. However, given the reduced relevance of data statistics in video-related OPs, our analysis centers on the correlations among the 16 VBench evaluation metrics. These metrics are clustered into three groups, with the best-performing OP selected from each group.

Through OP combination experiments, we pinpoint the most effective set of OPs. We then sample 40k instances from the filtered data pool and repeat the training process for up to 10 epochs. For comparative analysis, we adhere to the method outlined in Section 3.3.3, selecting larger data volumes (80k, 120k, ..., up to 400k instances) for single-epoch training. This exploration also leads to valuable insights for optimizing text-to-video model training, especially on informed decisions of data filtering OPs and ideal iteration counts.

Across all experiments, results are reported as averages from 2 to 5 repetitions, inclusive of standard deviations. Detailed training configurations, performance metrics, and OP descriptions are provided in the Appendix A.

5 MAIN RESULTS AND INSIGHTS

In this section, we show the results of the specific applications of the probe-analyze-refine workflow that we proposed for data-model co-development in image-to-text and text-to-video generation (Section 4). Initially, by conducting experiments with individual operators, we investigate the impact of different data selection strategies on the model, summarizing fundamental insights (Section 5.1). Subsequently, building on this foundation, we select suitable candidate operators for combination experiments to identify the appropriate recipe (Section 5.2). After discovering this recipe, we construct a data pyramid hierarchy to explore whether to reuse high-quality data or sacrifice quality for increased data diversity (Section 5.3). Finally, leveraging the insights gained, we scale up the data and model to train high-quality models (Section 5.4).

Due to the space limitation, we present main conclusions and defer complete numeric results and details in Appendix B. Specifically, for the image-to-text generation, we mainly report the increase in average performance relative to the baseline on TextVQA (Singh et al., 2019), MMBench (Liu et al., 2023), and MME (Fu et al., 2023). For the text-to-video generation, we report the improvement in

Task	OP-Generated Statistics	Average Performance Changes (%)		
		Data Pool (Low)	Data Pool (Mid)	Data Pool (High)
Image-to-Text	Image NSFW Score	7.13 ± 4.29	18.44 ± 18.45	66.38 ± 32.65
	Text Action Number	59.90 ± 46.49	0.29 ± 2.16	-2.05 ± 2.48
	Language Score	49.90 ± 53.82	0.85 ± 2.87	-1.43 ± 2.40
	CLIP Image-Text Similarity	1.20 ± 4.86	-1.81 ± 2.88	49.81 ± 44.72
	Phrase Grounding Recall	-0.49 ± 3.87	-0.58 ± 6.12	49.39 ± 29.83
	Image Width	42.04 ± 57.27	10.31 ± 12.59	1.35 ± 4.36
	Special Character Ratio	-3.08 ± 0.63	-0.75 ± 1.61	39.67 ± 58.82
	Flagged Word Ratio	38.48 ± 27.76	-0.39 ± 0.43	22.49 ± 29.81
	Image Height	35.66 ± 48.62	12.91 ± 10.42	18.73 ± 27.32
	Word Repetition Ratio	33.14 ± 23.39	2.59 ± 5.31	-0.55 ± 2.90
	Aesthetics Score	11.94 ± 12.21	16.58 ± 25.70	0.16 ± 3.67
Text-to-Video	Video Aesthetics Score	-0.98 ± 0.08	0.13 ± 0.09	0.96 ± 0.13
	Video NSFW Score	0.82 ± 0.36	-0.05 ± 0.07	-0.57 ± 0.07
	Frames-Text Similarity	-1.45 ± 0.69	0.23 ± 0.21	0.79 ± 0.15
	Special-Characters Ratio	0.54 ± 0.36	-0.13 ± 0.70	-0.14 ± 0.10
	Token Number	0.53 ± 0.04	0.18 ± 0.32	0.41 ± 0.25
	Video Height	-0.10 ± 0.21	0.12 ± 0.13	0.46 ± 0.44
	Video OCR-Area Ratio	0.44 ± 0.04	0.02 ± 0.63	-0.66 ± 0.23
	Word Number	-0.49 ± 0.07	-0.41 ± 0.72	0.44 ± 0.45
	Text Action Number	0.18 ± 0.56	-0.71 ± 0.28	0.37 ± 0.28
	Video Motion Score	-0.55 ± 0.40	0.33 ± 0.21	0.32 ± 0.15
	Video Aspect Ratio	-0.32 ± 0.14	0.11 ± 0.18	-0.02 ± 0.40
	Video Duration	-0.58 ± 0.05	-0.16 ± 0.09	0.04 ± 0.84

Table 1: The results for some investigated OPs gaining top performance and of particular interest, including their statistical dimensions and the average performance changes relative to the baseline. The training data pools are split with low, middle, and high statistical values for each OP. The training data pool for baseline is randomly sampled, and all compared pools are with equal data volume.

the average evaluation score on VBench (Huang et al., 2024). Please refer to Appendix A.2 for more details.

5.1 RANKING SINGLE-OPERATOR DATA POOLS

Table 1 illustrates the performance of some models trained on single-operator data pools, where the data processing OPs alongside others of particular interest. For a comprehensive analysis and detailed experimental results for each OP, please refer to Appendix B.1.

Observation 1

Generative models’ efficacy is intimately tied to the fidelity of modalities they are trained to generate, which can be explicitly reflected in filtering processes on training data.

Upon general observation, in the text-to-video generation, video-related OPs occupy the top performance ranks, with the first three OPs being video-related and presenting a notable gap over the fourth-ranked text-related OP. On the other hand, in the image-to-text generation, text-related OPs appear to be more influential.

Observation 2

Image-to-text models place greater emphasis on data diversity, whereas text-to-video models prioritize data quality.

A deeper analysis of Table 1 unveils that image-to-text models require a richer tapestry of data diversity compared to their text-to-video counterparts. For example, high-scoring images in terms of *NSFW (Not Safe For Work)* content and texts with lower *language scores* exhibit greater variety, areas where text-to-video models notably excel. Conversely, text-to-video models emphasize video quality, demonstrating superior performance with videos featuring minimal *NSFW* content. This preference aligns with the prevalent training practices for text-to-video models, which frequently incorporate random frame sampling techniques. This is evident in the pronounced variability in performance observed with extended video durations.

Observation 3

Dynamic information in the data poses a heightened learning challenge for image-to-text generation compared to text-to-video generation.

Moreover, considering the static nature of images, the image-to-text generation occasionally demands the parsing of dynamic content, compelling models to engage in a degree of creative inference for accurate interpretation and response. This challenge manifests in the difficulty image-to-text models encounter when confronted with data rich in dynamic information. As illustrated in Table 1, image-to-text models exhibit commendable performance with fewer *text actions*, while text-to-video models display opposing trends regarding *text action counts* and *video motion scores* within the video-text data.

Observation 4

A high degree of match between different modalities within the data is crucial for model performance in both image-to-text and text-to-video generation.

Finally, both image-to-text and text-to-video models exhibit a common affinity for a higher degree of alignment between modalities. This is substantiated by their exemplary performances in scenarios where measures of *image-text similarity*, *phrase grounding recall*, and *frames-text similarity* are high.

5.2 SHAPING DATA RECIPES OF TOP-3 OPERATOR COMBINATIONS

Based on the insights acquired from single OP experiments, we can combine OPs into recipes for data filtering to obtain higher-quality data. Figure 3 illustrates the performance changes brought by different recipe combinations compared to the baseline data pool.

Observation 5

The optimal data recipe does not necessarily result from combining the best individual OPs, nor does incorporating more high-performing OPs always lead to superior outcomes.

Given the exponential increase in possible OP combinations as the number of OPs grows, we focus on experimenting with combinations of three OPs at a time. An intuitive approach is to combine the top three OPs with the best overall performance from Table 1. However, as shown in Figure 3(a) and Figure 3(c), combining higher-performing OPs does not always yield better results, nor does adding more OPs guarantee improvement. For instance, in the image-to-text experiment depicted in Figure 3(a), the data pool with a high *image NSFW score*, although performing best in single-operator experiments, generally diminishes performance when combined with other pools. Similarly, in Figure 3(c), while pairwise combinations of OPs all show positive gains, integrating the best-performing OP into the combination of high *frames-text similarity* and low *video NSFW score* reduces the relative improvement over the baseline from 2.48% to 1.88%.

In addition to selecting the overall best-performing OPs, we aim to identify operators with distinct advantages to explore whether combining these operators can synergistically leverage their strengths for improved outcomes. We selected operators with unique strengths based on **correlation information** obtained from single-operator experiments. Detailed correlation analyses can be found in Appendix B.2.

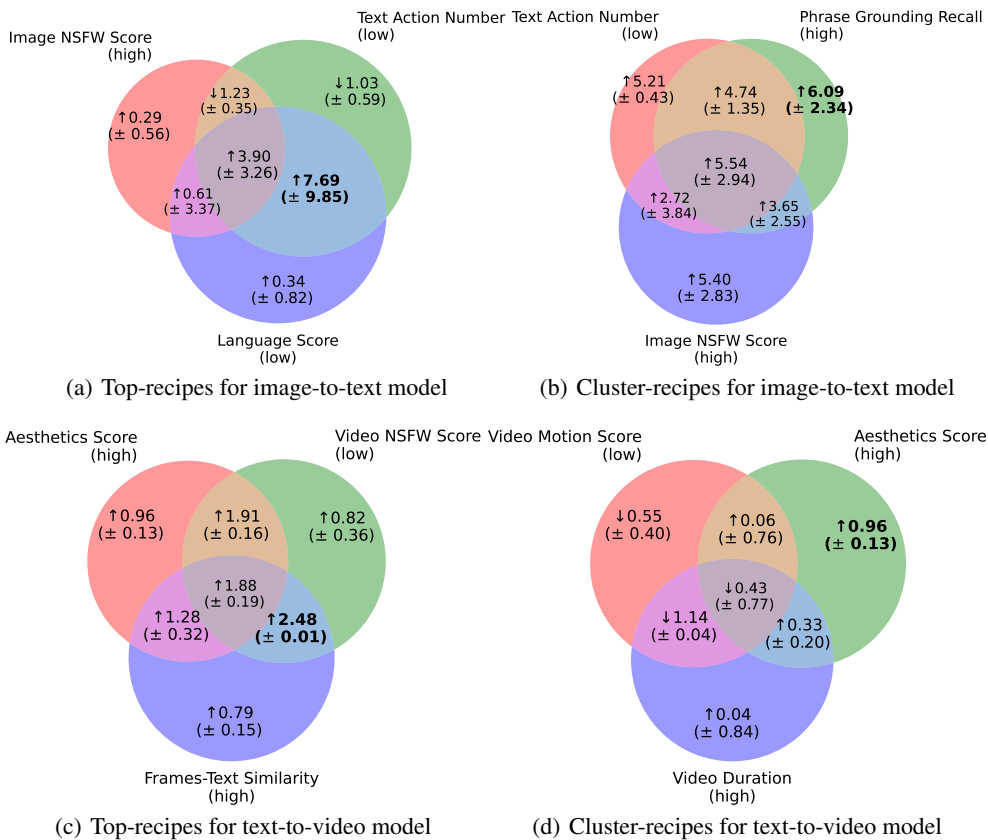


Figure 3: The improvements (%) of recipes with different OP combinations. The top recipes are derived from the combinations of the top-3 overall OPs listed in Table 1, whereas the cluster recipes stem from the combinations of the best OPs in 3 categories. These categories are based on correlation coefficients, as described in Section 4.1 and Section 4.2. In the image-to-text generation, due to the limited data volume in the top-level data pool, the amount of data used for training in the top-recipes decreased from 240k to 159k, and in the cluster-recipes, it dropped to 126k.

Specifically, for the image-to-text generation, we categorize the OPs by calculating correlations between their statistics. We then select representative operators within each category: `TextActionFilter` for text, `ImageNSFWFilter` for images, and `PhraseGroundingRecallFilter` for combined text-image relevance. For the text-to-video generation, based on single-operator experiments, we categorize the metrics of VBench (Huang et al., 2024) into three classes according to their relevance and select the best-performing operator from each category. The chosen operators are `VideoMotionScoreFilter`, which excels in video static features; `VideoDurationFilter`, which is superior in dynamic features; and `VideoAestheticsFilter`, which exhibits the best composite performance in video quality and video-text matching. We summarize the experiments results in Figure 3(b).

Observation 6

Combining OPs that excel in orthogonal dimensions on model or data does not guarantee complementary effects; rather, it is more likely that they will impede each other’s performance.

As depicted in Figure 3(b), regardless of how these top-performing OPs are combined, they ultimately reduce the model’s performance in both image-to-text and text-to-video generation. This observation challenges the naive assumption widely used in existing SOTA works, that various intuitively useful data cleansing actions, when stacked serially, can synergistically enhance performance.

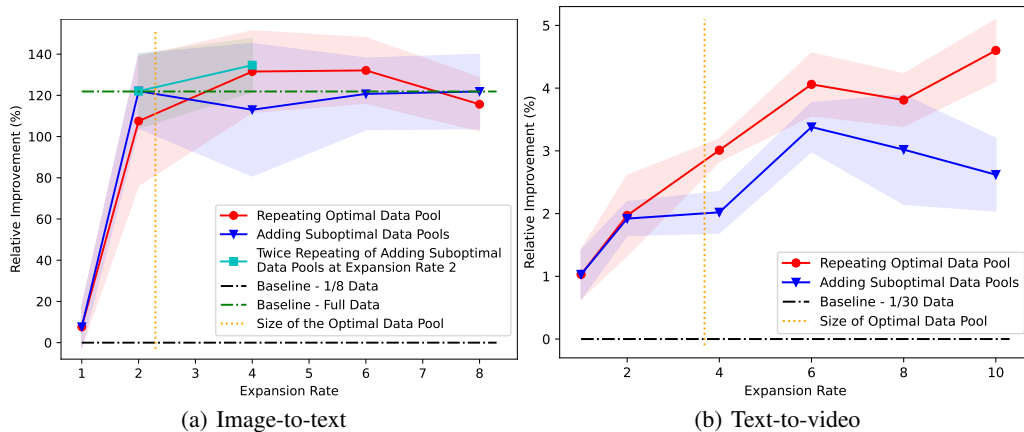


Figure 4: Relative improvement over the baseline for both image-to-text and text-to-video models is observed when these are trained on repeated top data pools and when additional suboptimal data pools are included. In the latter strategy, data sampling begins with the optimal data pool and, if necessary due to insufficient volume, continues by progressively sourcing from suboptimal data pools based on the pyramid hierarchy in Figure 3.

Observation 7

The performance of a single OP is positively correlated with the performance of the recipe created from its combination. Starting with high-performing OPs is a good initial step in exploring optimal higher-order data recipes.

Although the Top-3 operator recipes exhibit suboptimal performance, we observe positive gains when combining the top-2 operators, outperforming both single top-1 and top-3 combinations. For example, combining `TextActionFilter` and `LanguageIDScoreFilter` for the image-to-text generation, as well as `VideoNSFWFilter` and `VideoFramesTextSimilarityFilter` for the text-to-video generation, has proven to be highly effective.

5.3 HARNESSING MORE HIGH-QUALITY DATA

As discussed in Section 3.3.3 and illustrated in Figure 3, we can construct pyramid-shaped data pools by combining different OPs. Figure 3 provides specific performance metrics for each pool within this pyramid structure. The best-quality data often resides at the higher levels of the pool; however, these levels also contain less data. Therefore, during model training, it is crucial to determine when to reuse high-quality data and when to introduce suboptimal data to ensure diversity. The experiments in this section are designed to address this question.

In these experiments, we select the best-performing data pool from Figure 3 as the optimal data pool. Specifically, for the image-to-text model, we select the data pool with a low *text action number* and a high *language score*, and for the text-to-video model, we choose the data pool with a low *video NSFW score* and a high *frames-text similarity*. We also adhere to the setup in Figure 3, where the baseline for image-to-text trains on 159k data instances, and the baseline for text-to-video trains on 40k data instances.

Observation 8

Duplicating high-quality data is beneficial for both image-to-text and text-to-video models. For the image-to-text model, optimal utilization of high-quality data may be achieved after four repetitions, while for the text-to-video model, it is effective to reuse high-quality data extensively between six to ten times.

For the text-to-video model (Figure 4(b)), when the expansion rate equals 2, the performance utilizing data repeated twice is comparable to training with double the data volume from the optimal data pool, indicating that reusing the data twice does not adversely impact the model’s performance. The line graph from the repeating top data pool experiment demonstrates that this trend continues up to six repetitions, during which the model’s performance steadily increases linearly. After six repetitions, some negative impacts on the model’s performance begin to appear, but improvements are still observed even after ten repetitions, suggesting the negative impact is not particularly strong. By contrast, for the image-to-text model (Figure 4(a)), when data is repeated twice compared to using double the amount of optimal data, there is a 15% reduction in relative improvement. Moreover, the benefits of reusing this data diminish significantly with further repetitions, and negative impacts emerge when the data is repeated eight times.

In Figure 4(b), compared to reusing high-quality data, the negative impact of introducing suboptimal data is evident. At an expansion rate of 4, the experiment adding suboptimal data pools shows a significant performance drop compared to repeating quality data, even though suboptimal data only accounts for 8%. Although at an expansion rate of 6, the diversity of the data plays a certain role, the model’s performance continues to decline as the proportion of suboptimal data increases at higher expansion rates. Experiments conducted on the image-to-text model also emphasize the importance of data quality. As shown in Figure 4(a), the model’s performance did not improve after incorporating suboptimal data.

This suggests that the text-to-video model exhibits a higher tolerance for data diversity compared to the image-to-text model, yet both models underscore the critical importance of data quality. This observation aligns with our findings in Section 5.1 and based on our observations of the impact of video duration on the model, we hypothesize that this may be related to the model’s training involving random frame sampling from videos.

5.4 APPLYING DATA-MODEL INSIGHTS IN LARGER-SCALE SCENARIOS

In this section, we apply the insights gained from the previous experiments to larger-scale models and datasets. Specifically, in line with the best data recipe from Figure 3 and Observation 7, we scale up data pool on the full-size candidate video datasets introduced in Section 4, with low video NSFW scores and high frame-text similarities, encompassing approximately 147k instances. Additionally, following Observation 8, we set epochs to 6, running the data through the model for six passes of training. From the data development view, this transition allows us to probe the scalability of our methodologies, advancing from the 40k data pool used in Section 5 to a significantly more voluminous dataset, approximately $22\times$ larger. From the model development view, we undertake a stringent challenge to assess the transferability of our findings across different model architectures, by replacing the training model from previous EasyAnimate into another SOTA model, T2V-Turbo (Li et al., 2024).

Table 2 showcases our notable achievements on the VBench leaderboard², achieving a new SOTA. Compared to our baseline model, T2V-Turbo, our method yields a notable uplift of 1.09% on the *Board Average* score, with the *Quality Average* score experiencing a boost of 0.57%, and a particularly pronounced elevation in the *Semantic Average* score, which escalates by 3.17%. This underscores the pivotal role played by our proposed data-model refinement strategies within this context. The `VideoFramesTextSimilarityFilter` effectively bolsters the alignment between the generated videos and the corresponding prompts, while the `VideoNSFWFilter` safeguards the maintenance of high video generation quality standards. It is also worth highlighting that our approach charts a novel trajectory for the advancement of text-to-video models. While both T2V-Turbo and VEnhancer embody architectural refinements building upon the foundation of VideoCrafter-2.0, our methodology augments T2V-Turbo’s performance through a synergistic data-model co-development workflow. For exhaustive experimental setups and supplementary ablation studies concerning T2V-Turbo, readers are directed to Appendix B.3.

²The leaderboard is accessible at VBench Online Portal.

Models (Ranked by leaderboard)	Board Avg. (%)	Uniform Avg. (%)	Quality Avg. (%)	Semantic Avg. (%)
1. Data-Juicer (T2V)	82.10	80.54	83.14	77.93
2. VEnhancer (VC2) (He et al., 2024a)	81.97	80.00	83.27	76.73
3. LaVie-2 (Wang et al., 2023a)	81.75	79.50	83.24	75.76
4. T2V-Turbo (VC2) (Li et al., 2024)	81.01	78.67	82.57	74.76
5. Gen-2 (Esser et al., 2023)	80.58	80.11	82.47	77.75
6. VideoCrafter-2.0 (Chen et al., 2024b)	80.44	77.81	82.20	73.42
7. Pika Beta (2023-06) (Pika)	80.40	76.97	82.68	71.26
8. AnimateDiff-V2 (Guo et al., 2024)	80.27	76.33	82.90	69.75

Table 2: Leading models on the VBench leaderboard as of July 16, 2024, as recorded in Figure 5 in Appendix. “Board Avg.” denotes the weighted average of normalized scores across 16 metrics defined by VBench. “Quality Avg.” represents the aggregated scores from 7 video quality metrics, whereas “Semantic Avg” aggregates scores from 9 metrics evaluating the consistency between prompts and generated videos. “Uniform Avg.” indicates the simple average of scores related to quality and semantic metrics.

6 CONCLUSIONS

In this paper, we introduced the Data-Juicer Sandbox, a pioneering open-source suite designed to facilitate the collaborative development of multi-modal data and generative models. By integrating a flexible and comprehensive array of customizable components at different levels, our sandbox enables systematic, cost-effective exploration and optimization, effectively bridging the often-disjointed domains of data and model development. Through the implementation of a “Probe-Analyze-Refine” workflow, we showcased how our sandbox can yield not only significant improvements in both dataset and trained models, but also valuable insights into the complex interplay between data preprocessing and model performance.

Looking ahead, we will continuously extend the sandbox’s compatibility to encompass a broader range of model-centric infrastructures and develop more off-the-shelf and effect-proven workflows, to facilitate reuse and expedite innovation. Besides, recognizing the growing capabilities of generative models in synthesizing data, it is also a crucial direction to investigate the ethical implications of data processing choices and their downstream effects on model outputs.

REFERENCES

- Tianyi Bai, Hao Liang, Binwang Wan, Ling Yang, Bozhou Li, Yifan Wang, Bin Cui, Conghui He, Binhang Yuan, and Wentao Zhang. A survey of multimodal large language model from a data-centric perspective. *arXiv preprint arXiv:2405.16640*, 2024.
- Max Bain, Arsha Nagraani, Gül Varol, and Andrew Zisserman. Frozen in time: A joint video and image encoder for end-to-end retrieval. In *Proceedings of the IEEE/CVF international conference on computer vision*, pp. 1728–1738, 2021.
- G. Bradski. The OpenCV Library. *Dr. Dobb’s Journal of Software Tools*, 2000.
- Davide Caffagni, Federico Cocchi, Luca Barsellotti, Nicholas Moratelli, Sara Sarto, Lorenzo Baraldi, Lorenzo Baraldi, Marcella Cornia, and Rita Cucchiara. The (r)evolution of multimodal large language models: A survey, 2024.
- Daoyuan Chen, Yilun Huang, Zhijian Ma, Heseng Chen, Xuchen Pan, Ce Ge, Dawei Gao, Yuexiang Xie, Zhaoyang Liu, Jinyang Gao, Yaliang Li, Bolin Ding, and Jingren Zhou. Data-juicer: A one-stop data processing system for large language models. In *International Conference on Management of Data (SIGMOD)*, 2024a.
- Haoxin Chen, Yong Zhang, Xiaodong Cun, Menghan Xia, Xintao Wang, Chao Weng, and Ying Shan. Videocrafter2: Overcoming data limitations for high-quality video diffusion models, 2024b.
- Tsai-Shien Chen, Aliaksandr Siarohin, Willi Menapace, Ekaterina Deyneka, Hsiang-wei Chao, Byung Eun Jeon, Yuwei Fang, Hsin-Ying Lee, Jian Ren, Ming-Hsuan Yang, and Sergey Tulyakov. Panda-70m: Captioning 70m videos with multiple cross-modality teachers. *arXiv preprint arXiv:2402.19479*, 2024c.
- Together Computer. Redpajama: an open dataset for training large language models, October 2023. URL <https://github.com/togethercomputer/RedPajama-Data>.
- Grégoire Delétang, Anian Ruoss, Paul-Ambroise Duquenne, Elliot Catt, Tim Genewein, Christopher Mattern, Jordi Grau-Moya, Li Kevin Wenliang, Matthew Aitchison, Laurent Orseau, Marcus Hutter, and Joel Veness. Language modeling is compression, 2024.
- Ruofei Du, Na Li, Jing Jin, Michelle Carney, Scott Miles, Maria Kleiner, Xiuxiu Yuan, Yinda Zhang, Anuva Kulkarni, Xingyu Liu, et al. Rapsai: Accelerating machine learning prototyping of multimedia applications through visual programming. In *Proceedings of the 2023 CHI Conference on Human Factors in Computing Systems*, pp. 1–23, 2023.
- Patrick Esser, Johnathan Chiu, Parmida Atighehchian, Jonathan Granskog, and Anastasis Germanidis. Structure and content-guided video synthesis with diffusion models. In *Proceedings of the IEEE/CVF International Conference on Computer Vision*, pp. 7346–7356, 2023.
- Chaoyou Fu, Peixian Chen, Yunhang Shen, Yulei Qin, Mengdan Zhang, Xu Lin, Jinrui Yang, Xiawu Zheng, Ke Li, Xing Sun, et al. Mme: A comprehensive evaluation benchmark for multimodal large language models. *arXiv preprint arXiv:2306.13394*, 2023.
- Ce Ge, Zhijian Ma, Daoyuan Chen, Yaliang Li, and Bolin Ding. Data mixing made efficient: A bivariate scaling law for language model pretraining, 2024. URL <https://arxiv.org/abs/2405.14908>.
- Yuwei Guo, Ceyuan Yang, Anyi Rao, Zhengyang Liang, Yaohui Wang, Yu Qiao, Maneesh Agrawala, Dahua Lin, and Bo Dai. Animatediff: Animate your personalized text-to-image diffusion models without specific tuning. *International Conference on Learning Representations*, 2024.
- Eric Harper, Somshubra Majumdar, Oleksii Kuchaiev, Li Jason, Yang Zhang, Evelina Bakhturina, Vahid Noroozi, Sandeep Subramanian, Koluguri Nithin, Huang Jocelyn, Fei Jia, Jagadeesh Balam, Xuesong Yang, Micha Livne, Yi Dong, Sean Naren, and Boris Ginsburg. NeMo: a toolkit for Conversational AI and Large Language Models. URL <https://github.com/NVIDIA/NeMo>.

-
- Jingwen He, Tianfan Xue, Dongyang Liu, Xinqi Lin, Peng Gao, Dahua Lin, Yu Qiao, Wanli Ouyang, and Ziwei Liu. Venhancer: Generative space-time enhancement for video generation. *arXiv preprint arXiv:2407.07667*, 2024a.
- Muyang He, Yexin Liu, Boya Wu, Jianhao Yuan, Yuezhe Wang, Tiejun Huang, and Bo Zhao. Efficient multimodal learning from data-centric perspective. *arXiv preprint arXiv:2402.11530*, 2024b.
- Edward J Hu, Yelong Shen, Phillip Wallis, Zeyuan Allen-Zhu, Yanzhi Li, Shean Wang, Lu Wang, and Weizhu Chen. Lora: Low-rank adaptation of large language models. *arXiv preprint arXiv:2106.09685*, 2021.
- Ziqi Huang, Yanan He, Jiashuo Yu, Fan Zhang, Chenyang Si, Yuming Jiang, Yuanhan Zhang, Tianxing Wu, Qingyang Jin, Nattapol Chanpaisit, et al. Vbench: Comprehensive benchmark suite for video generative models. In *Proceedings of the IEEE/CVF Conference on Computer Vision and Pattern Recognition*, pp. 21807–21818, 2024.
- Jeff Hwang, Moto Hira, Caroline Chen, Xiaohui Zhang, Zhaoheng Ni, Guangzhi Sun, Pingchuan Ma, Ruizhe Huang, Vineel Pratap, Yuekai Zhang, Anurag Kumar, Chin-Yun Yu, Chuang Zhu, Chunxi Liu, Jacob Kahn, Mirco Ravanelli, Peng Sun, Shinji Watanabe, Yangyang Shi, Yumeng Tao, Robin Scheibler, Samuele Cornell, Sean Kim, and Stavros Petridis. Torchaudio 2.1: Advancing speech recognition, self-supervised learning, and audio processing components for pytorch, 2023.
- Johannes Jakubik, Michael Vössing, Niklas Kühnl, Jannis Walk, and Gerhard Satzger. Data-centric artificial intelligence. *Business & Information Systems Engineering*, pp. 1–9, 2024.
- Qirui Jiao, Daoyuan Chen, Yilun Huang, Yaliang Li, and Ying Shen. Enhancing multimodal large language models with vision detection models: An empirical study. *arXiv preprint arXiv:2401.17981*, 2024.
- Quentin Lhoest, Albert Villanova del Moral, Yacine Jernite, Abhishek Thakur, Patrick von Platen, Suraj Patil, Julien Chaumond, Mariama Drame, Julien Plu, Lewis Tunstall, Joe Davison, Mario Šaško, Gunjan Chhablani, Bhavitvya Malik, Simon Brandeis, Teven Le Scao, Victor Sanh, Canwen Xu, Nicolas Patry, Angelina McMillan-Major, Philipp Schmid, Sylvain Gugger, Clément Delangue, Théo Matussière, Lysandre Debut, Stas Bekman, Pierric Cistac, Thibault Goehringer, Victor Mustar, François Lagunas, Alexander Rush, and Thomas Wolf. Datasets: A community library for natural language processing. In *Proceedings of the 2021 Conference on Empirical Methods in Natural Language Processing: System Demonstrations*, pp. 175–184, Online and Punta Cana, Dominican Republic, November 2021. Association for Computational Linguistics. URL <https://aclanthology.org/2021.emnlp-demo.21>.
- Jiachen Li, Weixi Feng, Wenhui Chen, and William Yang Wang. Reward guided latent consistency distillation, 2024.
- Yanwei Li, Yuechen Zhang, Chengyao Wang, Zhisheng Zhong, Yixin Chen, Ruihang Chu, Shaoteng Liu, and Jiaya Jia. Mini-gemini: Mining the potential of multi-modality vision language models. *arXiv:2403.18814*, 2023.
- Mengsha Liu, Daoyuan Chen, Yaliang Li, Guian Fang, and Ying Shen. Chartthinker: A contextual chain-of-thought approach to optimized chart summarization. In *Proceedings of the International Conference on Computational Linguistics (COLING)*, 2024a.
- Yuan Liu, Haodong Duan, Yuanhan Zhang, Bo Li, Songyang Zhang, Wangbo Zhao, Yike Yuan, Jiaqi Wang, Conghui He, Ziwei Liu, et al. Mmbench: Is your multi-modal model an all-around player? *arXiv preprint arXiv:2307.06281*, 2023.
- Yuan Liu, Haodong Duan, Yuanhan Zhang, Bo Li, Songyang Zhang, Wangbo Zhao, Yike Yuan, Jiaqi Wang, Conghui He, Ziwei Liu, Kai Chen, and Dahua Lin. Mmbench: Is your multi-modal model an all-around player?, 2024b. URL <https://arxiv.org/abs/2307.06281>.
- Lin Long, Rui Wang, Ruixuan Xiao, Junbo Zhao, Xiao Ding, Gang Chen, and Haobo Wang. On LLMs-driven synthetic data generation, curation, and evaluation: A survey. *arXiv preprint arXiv:2406.15126*, 2024.

-
- Laura Manduchi, Kushagra Pandey, Robert Bamler, Ryan Cotterell, Sina Däubener, Sophie Fellenz, Asja Fischer, Thomas Gärtner, Matthias Kirchler, Marius Kloft, Yingzhen Li, Christoph Lippert, Gerard de Melo, Eric Nalisnick, Björn Ommer, Rajesh Ranganath, Maja Rudolph, Karen Ullrich, Guy Van den Broeck, Julia E Vogt, Yixin Wang, Florian Wenzel, Frank Wood, Stephan Mandt, and Vincent Fortuin. On the challenges and opportunities in generative ai, 2024.
- MMagic Contributors. MMagic: OpenMMLab multimodal advanced, generative, and intelligent creation toolbox. <https://github.com/open-mmlab/mmagic>, 2023.
- OpenAI. GPT-4 technical report. *CoRR*, abs/2303.08774, 2023.
- OpenAI. Hello gpt-4o. <https://openai.com/index/hello-gpt-4o/>, 2024a.
- OpenAI. Sora: Creating video from text. <https://openai.com/sora>, 2024b.
- Yifan Peng, Jinchuan Tian, Brian Yan, Dan Berrebbi, Xuankai Chang, Xinjian Li, Jiatong Shi, Siddhant Arora, William Chen, Roshan Sharma, et al. Reproducing whisper-style training using an open-source toolkit and publicly available data. *arXiv preprint arXiv:2309.13876*, 2023.
- Pika. Pika art website. <https://pika.art/>.
- Zhen Qin, Daoyuan Chen, Wenhao Zhang, Liuyi Yao, Yilun Huang, Bolin Ding, Yaliang Li, and Shuiguang Deng. The synergy between data and multi-modal large language models: A survey from co-development perspective, 2024. URL <https://arxiv.org/abs/2407.08583>.
- Amanpreet Singh, Vivek Natarajan, Meet Shah, Yu Jiang, Xinlei Chen, Dhruv Batra, Devi Parikh, and Marcus Rohrbach. Towards vqa models that can read. In *Proceedings of the IEEE/CVF conference on computer vision and pattern recognition*, pp. 8317–8326, 2019.
- Thomas Unterthiner, Sjoerd van Steenkiste, Karol Kurach, Raphaël Marinier, Marcin Michalski, and Sylvain Gelly. FVD: A new metric for video generation. In *Deep Generative Models for Highly Structured Data, ICLR 2019 Workshop*, 2019.
- Patrick von Platen, Suraj Patil, Anton Lozhkov, Pedro Cuenca, Nathan Lambert, Kashif Rasul, Mishig Davaadorj, Dhruv Nair, Sayak Paul, William Berman, Yiyi Xu, Steven Liu, and Thomas Wolf. Diffusers: State-of-the-art diffusion models. <https://github.com/huggingface/diffusers>, 2022.
- Yaohui Wang, Xinyuan Chen, Xin Ma, Shangchen Zhou, Ziqi Huang, Yi Wang, Ceyuan Yang, Yanan He, Jiashuo Yu, Peiqing Yang, et al. Lavie: High-quality video generation with cascaded latent diffusion models. *arXiv preprint arXiv:2309.15103*, 2023a.
- Yi Wang, Yanan He, Yizhuo Li, Kunchang Li, Jiashuo Yu, Xin Ma, Xinhao Li, Guo Chen, Xinyuan Chen, Yaohui Wang, Conghui He, Ping Luo, Ziwei Liu, Yali Wang, Limin Wang, and Yu Qiao. Internvid: A large-scale video-text dataset for multimodal understanding and generation. *arXiv preprint arXiv:2307.06942*, 2023b.
- Yiqi Wang, Wentao Chen, Xiaotian Han, Xudong Lin, Haiteng Zhao, Yongfei Liu, Bohan Zhai, Jianbo Yuan, Quanzeng You, and Hongxia Yang. Exploring the reasoning abilities of multimodal large language models (mllms): A comprehensive survey on emerging trends in multimodal reasoning, 2024.
- Thomas Wolf, Lysandre Debut, Victor Sanh, Julien Chaumond, Clement Delangue, Anthony Moi, Pierric Cistac, Tim Rault, Rémi Louf, Morgan Funtowicz, et al. Transformers: State-of-the-art natural language processing. In *Proceedings of the 2020 conference on empirical methods in natural language processing: system demonstrations*, pp. 38–45, 2020.
- Jiaqi Xu, Xinyi Zou, Kunzhe Huang, Yunkuo Chen, Bo Liu, MengLi Cheng, Xing Shi, and Jun Huang. Easyanimate: A high-performance long video generation method based on transformer architecture. *arXiv:2405.18991*, 2024a.
- Jun Xu, Tao Mei, Ting Yao, and Yong Rui. Msr-vtt: A large video description dataset for bridging video and language. In *Proceedings of the IEEE conference on computer vision and pattern recognition*, pp. 5288–5296, 2016.

Mengwei Xu, Wangsong Yin, Dongqi Cai, Rongjie Yi, Daliang Xu, Qipeng Wang, Bingyang Wu, Yihao Zhao, Chen Yang, Shihe Wang, Qiyang Zhang, Zhenyan Lu, Li Zhang, Shangguang Wang, Yuanchun Li, Yunxin Liu, Xin Jin, and Xuanzhe Liu. A survey of resource-efficient llm and multimodal foundation models, 2024b.

Peng Xu, Xiatian Zhu, and David A. Clifton. Multimodal learning with transformers: A survey. *IEEE Transactions on Pattern Analysis and Machine Intelligence*, 45(10):12113–12132, 2023. doi: 10.1109/TPAMI.2023.3275156.

Shukang Yin, Chaoyou Fu, Sirui Zhao, Ke Li, Xing Sun, Tong Xu, and Enhong Chen. A survey on multimodal large language models, 2024.

Duzhen Zhang, Yahan Yu, Chenxing Li, Jiahua Dong, Dan Su, Chenhui Chu, and Dong Yu. Mm-llms: Recent advances in multimodal large language models, 2024.

Pengyuan Zhou, Lin Wang, Zhi Liu, Yanbin Hao, Pan Hui, Sasu Tarkoma, and Jussi Kangasharju. A survey on generative ai and llm for video generation, understanding, and streaming, 2024.

APPENDIX

A DETAILED EXPERIMENTAL SETUPS

A.1 TRAINING CONFIGURATIONS

For the image-to-text generation, we conducted experiments on one of the state-of-the-art MLLMs, Mini-Gemini-2B (Li et al., 2023). We train the whole model from scratch with less training data (about 1/6 of the original training datasets) in baseline experiments to make sure each experiment can be finished within one day. We keep every training setting (e.g. learning rate scheduler, global batch size) the same as the original model except for training datasets and training devices. For single-OP and OP combination experiments are trained on only 1 A100 GPU for each experiment so we increase the number of gradient accumulation steps from 4 to 32 to keep the same global batch size. For experiments of duplicating high-quality datasets, 8 A100 GPUs are involved to train the model, and the number of gradient accumulation steps is restored to 4. Each experiment is repeated 3 times with different random seeds to make the final results more reliable.

For text-to-video generation, we adopt the advanced DiT-based EasyAnimate (Xu et al., 2024a) model, which integrates diverse datasets totaling 1,217k instances from InternVid (Wang et al., 2023b) (606k), Panda-70M (Chen et al., 2024c) (605k), and MSR-VTT (Xu et al., 2016) (6k). Baseline experiments are executed on a subset of 40k instances, employing LoRA (Hu et al., 2021) for efficiency. During training, we maintain a video resolution of 256x256, sample every other frame, and randomly select sequences of 16 consecutive frames. The training process involves performing a backward pass for the loss of every 8 samples, with single-OP and OP combination experiments trained on a single GPU with a batch size of 8 for 5k steps, amounting to approximately 16 GPU hours per training run. Experiments for duplicating high-quality data, as well as larger-scale training, are conducted with a batch size of 1 across 8 GPUs. The models employ the Adam optimizer for training, with a learning rate set to 2×10^{-5} , weight decay parameter at 3×10^{-2} , and epsilon configured to 10^{-10} . Each experiment is repeated twice with random seeds of 42 and 45, respectively.

A.2 PERFORMANCE METRICS

In the paper, we mainly report overall performance as the relative changes over the baseline in terms of the average across all model metrics with normalization as follows:

$$\frac{\sum_i^N s_i/N - \sum_i^N s'_i/N}{\sum_i^N s'_i/N} = \frac{\sum_i^N (s_i - s'_i)}{\sum_i^N s'_i}, \quad (3)$$

where N is the number of involved metrics, s_i is the score of i -th model measurement metric, s'_i is the corresponding score gained by the baseline model. Below are the specific evaluation metrics involved in this study.

TextVQA, MMBench, MME. These benchmarks serve as critical evaluators of MLLM’s proficiency in understanding images. TextVQA (Singh et al., 2019) specifically targets the assessment of MLLMs’ abilities to read and reason about textual content embedded within images. MMBench (Liu et al., 2023), a vast multimodal benchmark, encompasses perception and reasoning skills through a plethora of multi-choice questions, numbering in the thousands. Additionally, a Chinese translation, MMBench-CN, is integrated for broader accessibility. MME (Fu et al., 2023) focuses on the perceptual and cognitive competencies of MLLMs, incorporating 14 finely categorized subtasks, each addressing Yes/No inquiries underpinned by meticulously crafted guidelines.

VBench. We engage with VBench (Huang et al., 2024), a holistic benchmark suite tailored for the rigorous evaluation of video generative models. It facilitates granular and objective assessment across a spectrum of dimensions, deconstructing the concept of “video generation quality” into 16 discrete metrics. Each metric is assessed using a carefully curated suite of prompts, comprising 946 unique prompts, with the requirement to produce 5 videos per prompt.

Owing to the disparity in evaluation criteria and the inherent variability across different modalities, we discern that the magnitude of performance fluctuation in the image-to-text generation substantially exceeds that observed in the text-to-video generation. This discrepancy underscores again the need for nuanced data-model co-development in addressing the complexities inherent in each modality.

A.3 OPERATOR DESCRIPTIONS

The study involves a total of 31 operators (OPs) from Data-Juicer (Chen et al., 2024a), with their corresponding statistics and detailed descriptions provided in Table 3.

OP Name	Modality	Statistics	Description
alphanumeric_filter	text	Alphanumeric Ratio	Alphanumeric ratio in the text.
character_repetition_filter	text	Character Repetition Ratio	Char-level n-gram repetition ratio in text.
flagged_words_filter	text	Flagged Word Ratio	Flagged-word ratio in the text
image_aesthetics_filter	image	Image Aesthetics Score	Aesthetics score of the image
image_aspect_ratio_filter	image	Image Aspect Ratio	Aspect ratio of the image
image_nsfw_filter	image	Image NSFW Score	NSFW score of the image
image_shape_filter	image	Image Width/Height	Width and height of the image
image_size_filter	image	Image Size	Size in bytes of the image
image_text_matching_filter	text, image	BLIP Image-Text Similarity	Image-text classification matching score based on a BLIP model
image_text_similarity_filter	text, image	CLIP Image-Text Similarity	Image-text feature cosine similarity based on a BLIP model
image_watermark_filter	image	Image Watermark Score	Predicted watermark score of the image based on an image classification model
language_id_score_filter	text	Language Score	Predicted confidence score of the specified language
perplexity_filter	text	Text Perplexity	Perplexity score of the text
phrase_grounding_recall_filter	text, image	Phrase Grounding Recall	Locating recall of phrases extracted from text in the image
special_characters_filter	text	Special Character Ratio	Special character ratio in the text
stopwords_filter	text	Stopword Ratio	Stopword ratio in the text
text_action_filter	text	Text Action Number	Number of actions in the text
text_entity_dependency_filter	text	Entity Dependency Number	Number of dependency edges for an entity in the dependency tree of the text
text_length_filter	text	Text Length	Length of the text
token_num_filter	text	Token Number	Token number of the text
video_aesthetics_filter	video	Video Aesthetics Score	Aesthetics score of sampled frames in the video
video_aspect_ratio_filter	video	Video Aspect Ratio	Aspect ratio of the video
video_duration_filter	video	Video Duration	Duration of the video
video_frames_text_similarity_filter	text, video	Frames-Text Similarity	Similarities between sampled frames and text based on a CLIP/BLIP model
video_motion_score_filter	video	Video Motion Score	Motion score of the video
video_nsfw_filter	video	Video NSFW Score	NSFW score of the video
video_ocr_area_ratio_filter	video	Video OCR-Area Ratio	Detected text area ratio for sampled frames in the video
video_resolution_filter	video	Video Width/Height	Width and height of the video
video_watermark_filter	video	Video Watermark Score	Predicted watermark score of the sampled frames in the video based on an image classification model
words_num_filter	text	Word Number	Number of words in the text
word_repetition_filter	text	Word Repetition Ratio	Word-level n-gram repetition ratio in the text

Table 3: Overview of involved OPs in the study, including the modality they pertain to, along with their statistical data and detailed descriptions of these statistics.

B ADDITIONAL EXPERIMENTAL RESULTS

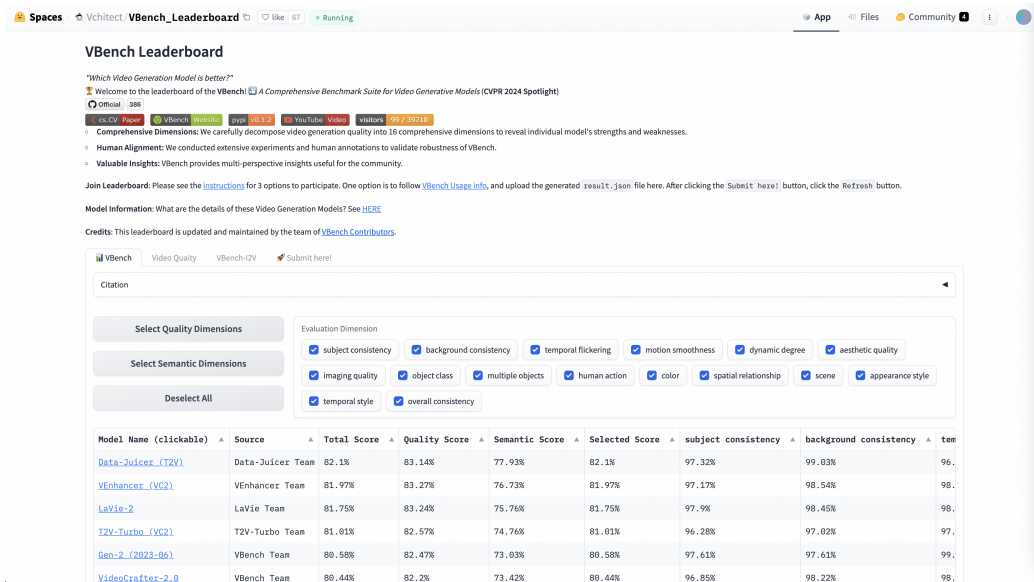


Figure 5: The VBench Leaderboard as of July 16, 2024, illustrating the rank 1 achievement empowered by our data-model co-development workflow.

B.1 COMPLETE OPERATOR RANKING

In Table 4, we present complete numeric results conducted on individual OP experiments (Section 5.1), from which we can discern some more detailed observations.

In image-to-text generation, it is preferable for the input of training images to align as closely as possible with the original configuration of the vision tower, such as training dimensions (height, width, sizes). Additionally, CLIP similarity scores tends to be more reliable than BLIP similarity scores. The BLIP similarity does not show much distinction and paradoxically, a lower similarity often results in better performance, which defies common sense. Images with excessively high aesthetic quality may offer limited assistance in feature alignment, while watermarks might have certain impacts on the OCR performance of the model.

In text-to-video generation, having a consistent aspect ratio for the training data is better than having ratios that are inconsistent but close to the 1:1 ratio used during training. For instance, a data pool with a 'middle' video aspect ratio consistently at 16:9 performs optimally. Videos with high video aesthetics scores and low video NSFW scores, as well as those with low video OCR-area ratios and high video motion scores, tend to be of higher quality. While single-text-related operators might not be as critical in text-to-video generation, they can still effectively filter out some dirty data.

B.2 CORRELATION ANALYSIS

In order to investigate the intrinsic relationships between OPs and to aid our recipe formulation, we observe relevance from following two perspectives.

Firstly, we adopt the most direct approach by examining the Pearson correlation coefficient between the statistics of OPs, as shown in Figures 6 for the image-to-text generation and Figures 7 for text-to-video generation. Intuitively, the associations between the statistics of OPs utilized in the image-to-text generation appear to be much stronger compared to those in the text-to-video generation. For example, in image-to-text generation, phrase grounding recall shows a strong positive correlation with text perplexity and special character ratio, while exhibiting a strong negative correlation with alphanumeric ratio, language score, text action number, stopword ratio, and text length. Meanwhile, in text-to-video generation, we only observe relationships between some of the purely textual OPs,

Task	OP-Generated Statistics	Average Performance Changes (%)		
		Data Pool (Low)	Data Pool (Mid)	Data Pool (High)
Image-to-Text	Image NSFW Score	7.13 ± 4.29	18.44 ± 18.45	66.38 ± 32.65
	Text Action Number	59.90 ± 46.49	0.29 ± 2.16	-2.05 ± 2.48
	Language Score	49.90 ± 53.82	0.85 ± 2.87	-1.43 ± 2.40
	CLIP Image-Text Similarity	1.20 ± 4.86	-1.81 ± 2.88	49.81 ± 44.72
	Phrase Grounding Recall	-0.49 ± 3.87	-0.58 ± 6.12	49.39 ± 29.83
	Image Width	42.04 ± 57.27	10.31 ± 12.59	1.35 ± 4.36
	Special Character Ratio	-3.08 ± 0.63	-0.75 ± 1.61	39.67 ± 58.82
	Flagged Word Ratio	38.48 ± 27.76	-0.39 ± 0.43	22.49 ± 29.81
	Image Height	35.66 ± 48.62	12.91 ± 10.42	18.73 ± 27.32
	Word Repetition Ratio	33.14 ± 23.39	2.59 ± 5.31	-0.55 ± 2.90
	Text Length	30.67 ± 28.54	-0.44 ± 0.73	-3.71 ± 0.39
	Stopword Ratio	3.34 ± 5.05	24.62 ± 36.73	-1.56 ± 1.59
	Image Size	0.76 ± 0.55	19.16 ± 27.29	1.58 ± 2.20
	Text Perplexity	-1.69 ± 1.30	16.70 ± 24.49	18.26 ± 23.02
	Image Aesthetics Score	11.94 ± 12.21	16.58 ± 25.70	0.16 ± 3.67
	Word Number	15.96 ± 29.01	-2.48 ± 0.26	-1.97 ± 2.05
	BLIP Image-Text Similarity	11.76 ± 22.83	1.74 ± 2.49	1.34 ± 2.21
	Image Watermark Score	-1.50 ± 2.41	7.51 ± 12.82	11.54 ± 13.14
	Alphanumeric Ratio	2.35 ± 7.63	-0.66 ± 0.69	8.71 ± 12.87
	Character Repetition Ratio	0.00 ± 1.13	-1.42 ± 0.60	7.94 ± 14.63
Entity Dependency Number	1.35 ± 1.81	-0.87 ± 1.15	6.67 ± 8.44	
Token Number	6.31 ± 7.86	0.80 ± 0.92	0.33 ± 6.45	
Image Aspect Ratio	0.00 ± 1.34	1.89 ± 2.71	-0.02 ± 1.12	
Text-to-Video	Video Aesthetics Score	-0.98 ± 0.08	0.13 ± 0.09	0.96 ± 0.13
	Video NSFW Score	0.82 ± 0.36	-0.05 ± 0.07	-0.57 ± 0.07
	Frames-Text Similarity	-1.45 ± 0.69	0.23 ± 0.21	0.79 ± 0.15
	Special-Characters Ratio	0.54 ± 0.36	-0.13 ± 0.70	-0.14 ± 0.10
	Token Number	0.53 ± 0.04	0.18 ± 0.32	0.41 ± 0.25
	Character Repetition Ratio	-0.29 ± 0.27	0.47 ± 0.80	0.18 ± -0.52
	Video Height	-0.10 ± 0.21	0.12 ± 0.13	0.46 ± 0.44
	Video OCR-Area Ratio	0.44 ± 0.04	0.02 ± 0.63	-0.66 ± 0.23
	Word Number	-0.49 ± 0.07	-0.41 ± 0.72	0.44 ± 0.45
	Entity Dependency Number	0.40 ± 0.01	0.28 ± 0.48	-0.18 ± 0.44
	Text Action Number	0.18 ± 0.56	-0.71 ± 0.28	0.37 ± 0.28
	Alphanumeric Ratio	-0.10 ± 0.19	0.20 ± 0.19	0.33 ± 0.17
	Video Motion Score	-0.55 ± 0.40	0.33 ± 0.21	0.32 ± 0.15
	Video Watermark Score	-0.27 ± 0.27	-0.25 ± 0.25	0.29 ± 0.16
	Text Perplexity	0.15 ± 0.69	-0.13 ± 0.27	0.09 ± 0.56
	Stopword Ratio	-0.01 ± 0.05	-0.48 ± 0.22	0.12 ± 0.07
	Video Aspect Ratio	-0.32 ± 0.14	0.11 ± 0.18	-0.02 ± 0.40
	Language Score	-0.21 ± 0.01	-0.03 ± 0.38	0.09 ± 0.03
	Word Repetition Ratio	0.00 ± 0.17	0.06 ± 0.24	-0.43 ± 0.24
	Video Duration	-0.58 ± 0.05	-0.16 ± 0.09	0.04 ± 0.84
Text Length	-0.09 ± 0.63	-0.66 ± 0.08	0.03 ± 0.22	

Table 4: The complete OP ranking, including their statistical dimensions and the improvements relative to the baseline. We consider three splits with low, middle, and high statistical values for each OP. The baseline used is based on random sampling with equal data volume.

with video-related operators being mostly orthogonal to the others. Therefore, for the image-to-text generation, we divide OPs into three categories based on the correlation of their statistics and select the optimal OP from each category to create combinations. However, this method does not seem quite appropriate for text-to-video generation, due to the sparser correlations observed.

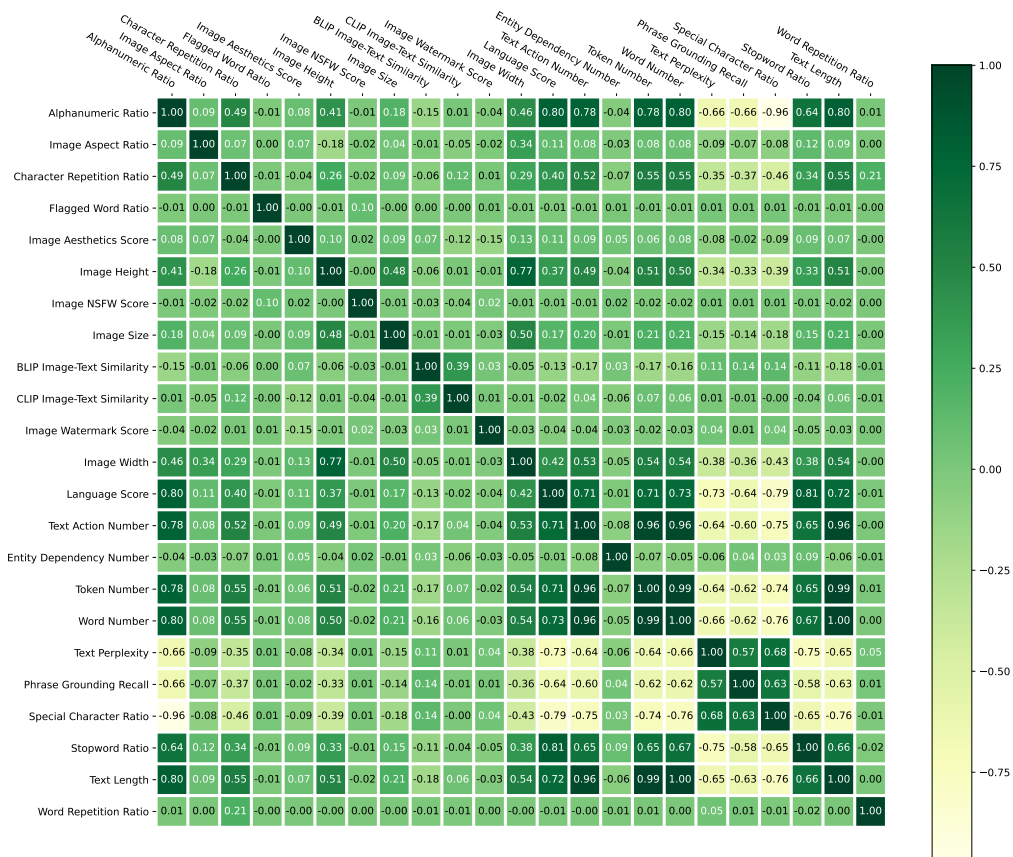


Figure 6: Pearson correlation coefficient of OP statistics from image-to-text generation.

In the second approach, we categorize the evaluation metrics based on their correlation, as illustrated in Figure 8 for the image-to-text generation and Figure 9 for the text-to-video generation. In the image-to-video generation, several evaluation metrics are quite specific and possess uniqueness, such as metrics for OCR and coding tasks, leading to a higher number of categories upon classification. In contrast, VBench’s evaluation metrics can easily be divided into several broad classes, which include static video metrics like subject and background consistency, dynamic metrics such as the dynamic degree, video quality indicators like aesthetic and imaging quality, as well as the degree of match between the generated video and the prompt, including object class and spatial relationship. The dynamic degree is particularly noteworthy as it negatively correlates with many other metrics and combats those that prefer static videos, thus preventing videos with no movement from being rated as optimal. Based on these observations, for the text-to-video generation, we apply a hierarchical clustering algorithm to divide VBench metrics into three categories based on their correlations, roughly classified into three types: static video metrics, dynamic video metrics, and video quality along with video-text matching. Subsequently, we select the best-performing OP for each of these three metric categories, where each excels in different aspects. These selected OPs are then combined and experimented with together.

B.3 SETTING AND ABLATION STUDY BASED ON T2V-TURBO

The results shown in Table 2 represent the enhancements we achieved based on T2V-Turbo (Li et al., 2024). T2V-Turbo applies LoRA (Hu et al., 2021) to VideoCrafter-2.0 (Chen et al., 2024b) and is trained on the WebVid (Bain et al., 2021) dataset, using VideoCrafter-2.0 as a teacher for distillation and incorporating reinforcement learning with rewards for the generated videos. We make the following cumulative modifications to T2V-Turbo:

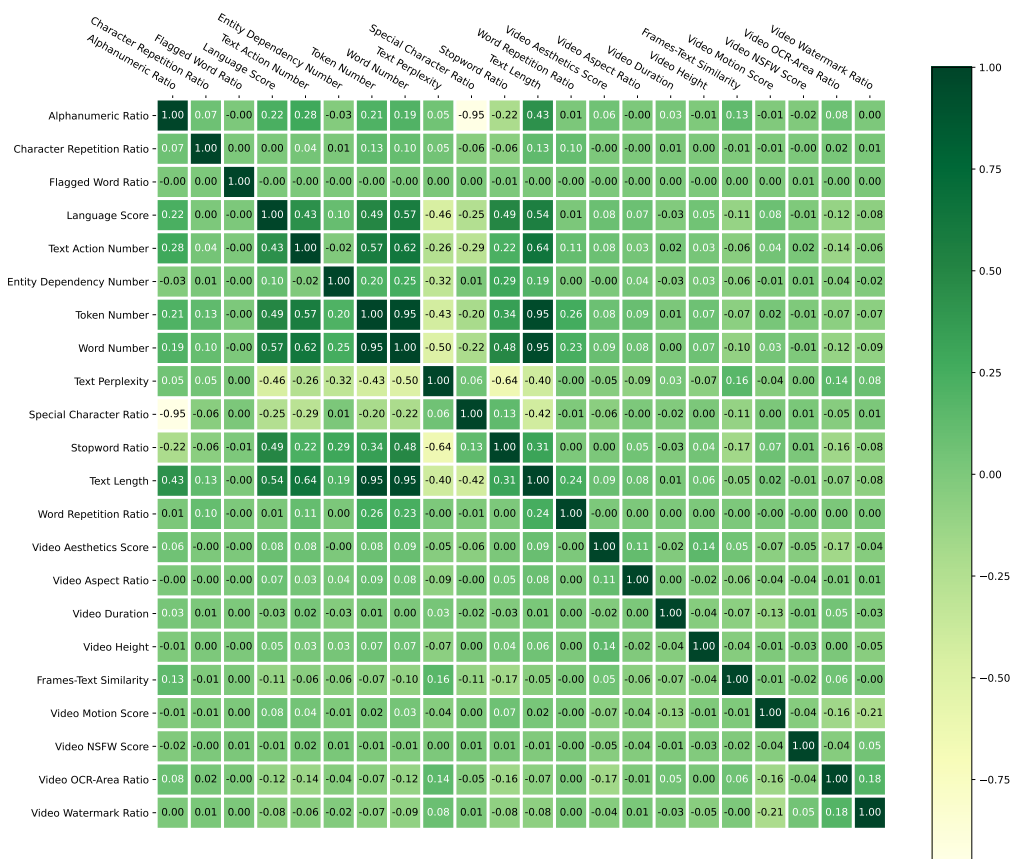


Figure 7: Pearson correlation coefficient of OP statistics from text-to-video generation.

- **Proposed Data Pool.** Utilizing the optimal data pool identified in Section 5.3, which consists of 147k instances with low video NSFW scores and high frame-text similarities, we replace the WebVid data and train for 6 epochs based on the insight from Section 5.3.
- **Initialization for LoRA.** We use the T2V-Turbo model to initialize the parameters for training with LoRA.
- **Self-Distillation.** When we initialize with the T2V-Turbo model, the student model is already outperforming the teacher model, VideoCrafter-2.0, potentially leading to unstable training. To mitigate this, we use the T2V-Turbo model itself as the teacher to ensure that the reinforcement learning does not diverge excessively.
- **Real-Data Loss.** To enhance the role of the proposed data pool during training, we add a real-data loss between the generated videos and the input videos to the distillation loss and reward loss. Furthermore, we set the weights of both the real-data loss and the distillation loss to 0.5.

Model	Total Score (%)	Quality Score (%)	Semantic Score (%)
T2V-Turbo (VC2)	81.01	82.57	74.76
+ Enhanced Data Pool	81.84	83.40	75.60
+ Initialization for LoRA	81.82	83.47	75.19
+ Self-Distillation	79.16	79.48	77.92
+ Real-Data Loss	82.10	83.14	77.93

Table 5: Our model undergoes ablation experiments on the VBench leaderboard evaluation. Each ‘+’ sign in the row indicates that the modification is added on top of the previous row’s configuration.

Table 5 presents the ablation experiments of our modifications in the VBench evaluation. It is clear that when we replace the WebVid data with our proposed data pool, the model experiences a notable

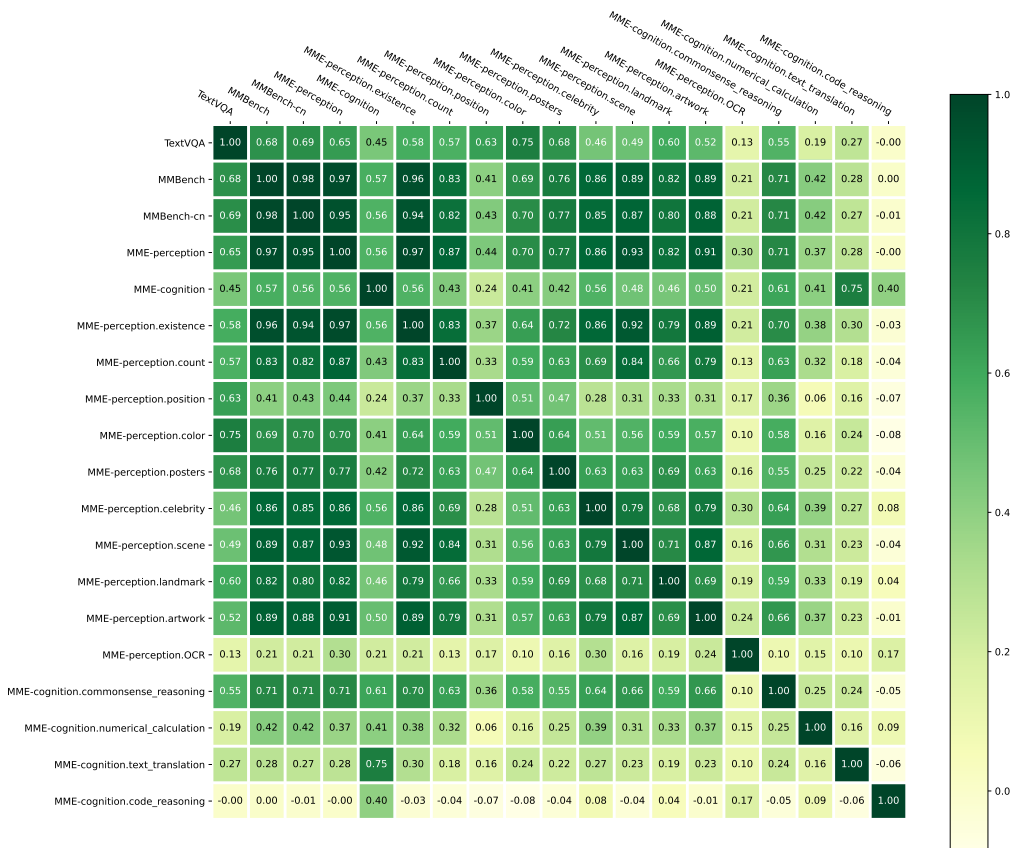


Figure 8: Pearson Correlation Coefficient of each dimension in TextVQA, MMBench, and MME

improvement, with the total score increasing from 81.01% to 81.84%. Subsequently, initializing the LoRA training parameters with the T2V-Turbo model does not lead to further enhancements in model performance. We suspect this might be because the teacher model is less effective than the T2V-Turbo model. Therefore, we use the T2V-Turbo model for self-distillation. While this method effectively raises the semantic score, it results in unstable video generation characterized by significant temporal flickering, which severely lowers the video quality. To counteract this, we add a real-data loss with the input data to secure the quality of the generated videos. Ultimately, while improving the semantic score, we ensure the video generation quality remains high and establish a new state-of-the-art.

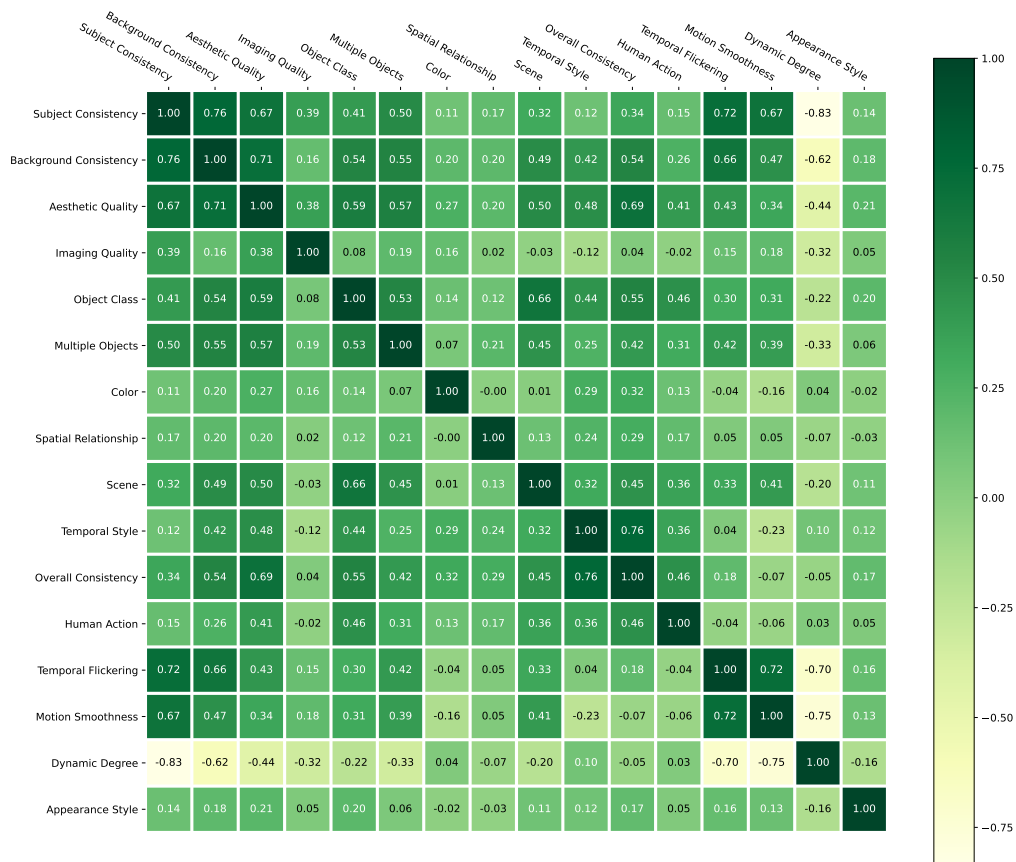


Figure 9: Pearson Correlation Coefficient of Evaluation Metrics of VBench